Room Temperature Polymorphism in Metastable $BiMnO_3$ Prepared by High-Pressure Synthesis

Erica Montanari,*,† Lara Righi,† Gianluca Calestani,†,‡ Andrea Migliori,§ Edmondo Gilioli,‡ and Fulvio Bolzoni‡

Dipartimento di Chimica GIAF, Università di Parma, Parco Area delle Scienze 17A, I-43100 Parma, CNR-IMM, Area della Ricerca di Bologna, Via Gobetti 101, I-40126 Bologna, and CNR-IMEM, Parco Area delle Scienze 37/A, I-43010 Parma, Italy

Received October 6, 2004. Revised Manuscript Received January 19, 2005

The $BiMnO_3$ perovskite is a very interesting multiferroic material that, once synthesized at high pressure and high temperature, survives as a metastable phase at ambient conditions. We investigated ceramic samples prepared in different conditions (temperature, pressure, and composition), and the existence of polymorphism at room temperature was clearly evidenced by electron diffraction and high-resolution electron microscopy in all the samples. A new polymorph, characterized by a different distortion of the perovskite basic cell, was found to coexist as a minor phase with the well-known C2 monoclinic form. The new polymorph, which can be described by a triclinic (pseudorhombohedral) superstructure with $a = 13.62$ Å, $b = 13.66$ Å, $c = 13.66$ Å, $\alpha = 110.0°$, $\beta = 108.8°$, and $\gamma = 108.8°$, is mostly segregated at the grain surface. Magnetic characterizations revealed for this second form a critical temperature of 107 K, a few degrees above the ferromagnetic transition of the monoclinic C2 form measured at 99 K. The new phase disappears by reheating the samples at ambient pressure, suggesting the idea of a higher energy polymorph, which kinetically converts in the usual phase once a sufficient temperature has been achieved.

Introduction

Bismuth manganite ($BiMnO_3$) has been widely investigated in the past few years, at first for its magnetic properties and then for its magnetoelectric multiferroic nature. In similar materials, ferroelectric and ferromagnetic order can coexist,[1] giving rise to unusual physical properties that open new perspectives in both scientific research and technological applications.[2,3]

$BiMnO_3$ has a perovskite-type structure and represents the high-pressure high-density phase in the ternary Bi−Mn−O system. Heating at ambient pressure a mixture of bismuth and manganese oxides in the correct ratio leads to $Bi_2Mn_4O_{10}$ and $Bi_{12}MnO_{20}$, whereas at high pressure (>40 kbar) the formation of the perovskite is favored. Recently, $BiMnO_3$ thin films were successfully grown on strontium titanate (STO) substrate by laser ablation, supplying a further example of the stabilization of a metastable perovskite by "lattice pressure" in the epitaxial growth.[4,5]

Despite its difficult synthesis, $BiMnO_3$ has been investigated since 1965,[6] mainly for its unexpected ferromagnetic behavior. Differently from $LaMnO_3$, which is an A-type antiferromagnetic manganite,[7] $BiMnO_3$ is a soft ferromagnetic material[8] with a Curie temperature (T_C) around 100 K. The particular magnetic behavior of $BiMnO_3$ is strictly related[9] to the stereoactive function of the $6s^2$ lone pair of the bismuth ion that plays a fundamental role in distorting the structure. Differently from rare-earth manganites, showing an orthorhombic distortion quite typical for the perovskite structure of several transition metals, bismuth manganite crystallizes in a highly distorted triclinic lattice[8] ($a \approx c \approx 3.935$ Å, $b \approx 3.989$ Å, $\alpha \approx \gamma \approx 91.46°$, and $\beta \approx 90.96°$). Ordering of partial empty d_{z^2} and $d_{x^2-y^2}$ orbitals of manganese ions was involved to explain the anomalous magnetic properties. A neutron powder diffraction experiment[10] gave evidence of a Jahn−Teller coherent distortion below magnetic transition, supporting this orbital ordering model.

The highly distorted $BiMnO_3$ structure is noncentrosymmetric and, as suggested by Hill,[11] exhibits ferroelectricity at room temperature. The ferroelectric Curie temperature has

* To whom correspondence should be addressed. Phone: +390521905447. Fax: +390521905556. E-mail: emontana@nemo.unipr.it.
† Università di Parma.
‡ CNR-IMEM.
§ CNR-IMM.

(1) Schmid, H. *Ferroelectrics* **1994**, *162*, 317.
(2) Freedman, A. J.; Schmid, H. *Magnetoelectric Interaction Phenomena in Crystals*; Gordon and Breach: London, 1975.
(3) Smolenskii, G. A.; Chupis, I. E. *Sov. Phys. Usp.* **1982**, *25*, 475.
(4) Moreira dos Santos, A. F.; Cheetham, A. K.; Tian, W.; Pan, X.; Jia, Y.; Murphy, N. J.; Lettieri, J.; Schlom, D. G. *Appl. Phys. Lett.* **2004**, *84*, 91.
(5) Ohshima, E.; Saya, Y.; Nantoh, M.; Kawai, M. *Solid State Commun.* **2000**, *116*, 73.
(6) Sugawara, F.; Iiida, S. *J. Phys. Soc. Jpn.* **1965**, *20*, 1529.
(7) Rao, C. N. R.; Cheetham, A. K.; Mahesh, R. *Chem. Mater.* **1996**, *8*, 2421.
(8) Sugawara, F.; Iiida, S.; Syono, Y.; Akimoto, S. *J. Phys. Soc. Jpn.* **1968**, *25*, 1553.
(9) Seshadri, R.; Hill, N. A. *Chem. Mater.* **2001**, *13*, 2892.
(10) Moreira dos Santos, A. F.; Cheetham, A. K.; Atou, T.; Syono, Y.; Yamaguchi, Y.; Ohoyama, K.; Chiba, H.; Rao, C. N. R. *Phys. Rev.* **2002**, *B66*, 064425.
(11) Hill, N. A. *J. Phys. Chem. B* **2000**, *104*, 6694. Hill, N. A.; Rabe, K. *Phys. Rev.* **1999**, *B59*, 8759.

10.1021/cm048250s CCC: $30.25
Published on Web 03/04/2005

been related to a structural phase transition occurring at 770 K.[12] Ferroelectric hysteresis loops were observed both in bulk and thin film samples.[13] Dos Santos et al.[13] and then Kimura et al.[12] proved the magnetoelectric multiferroic nature of $BiMnO_3$ in which ferroelectricity and ferromagnetism coexist below the ferromagnetic temperature, allowing magnetic control via an electric field (and vice versa). Large nonlinear optical properties, recently observed[14,15] in $BiMnO_3$ thin films, suggest possible interesting device applications.

Multiferroic materials are rare in nature. Whereas there are hundreds of compounds presenting magnetic or ferroelectric order, the physical/structural/chemical requests[11] for their coexistence are so hard that the number of multiferroic materials is dramatically reduced to a few cases. In such an interesting kind of material, the structural characterization is obviously extremely important. In 1998 Chiba et al.,[16] on the basis of electron diffraction (ED) and X-ray powder diffraction (XRPD) experiments, proposed a monoclinic superstructure, having $a = 9.54$ Å, $b = 5.61$ Å, $c = 9.86$ Å, and $\beta = 110.7°$, to justify the complex diffraction patterns of $BiMnO_3$. Taking into account the same unit cell, the crystal structure was refined in space group $C2$ by Atou et al.[17] in 1999 on the basis of powder neutron diffraction data. This structure, confirmed by further powder neutron diffraction studies,[10] is commonly accepted and used as a fundamental model for physical interpretation of the observed results.

The thermal evolution[12,18] at ambient pressure of $BiMnO_3$ has not been completely clarified. A reversible transition to a different monoclinic phase has been reported to occur at about 483 K, whereas an irreversible transition to a tetragonal or orthorhombic phase (connected with the ferroelectric−paraelectric transition) takes place at 770 K, followed by decomposition of the perovskite to a mixture of $Bi_2Mn_4O_{10}$ and Bi_2O_3. Neither the monoclinic nor the tetragonal (or orthorhombic) structure is known nowadays. Even at room temperature (and ambient pressure) the situation is far from being completely clarified. Just in the paper of Chiba et al.,[16] the existence of polymorphism at room temperature in $BiMnO_3$ samples prepared in high-pressure−high-temperature conditions was detected by ED. However, because the main peaks of X-ray or neutron powder diffraction patterns (always characterized by the presence of minor impurity phases) can be indexed on the basis of the commonly accepted monoclinic structure, the possible existence of polymorphism has been systematically ignored in all further papers. We decided to investigate the question by characterizing, from the structural and magnetic points of view, $BiMnO_3$ samples prepared in different conditions (temperature, pressure, and composition). The existence of polymorphism at room temperature was clearly evidenced by ED and high-resolution electron microscopy (HREM) in all the prepared samples, and the correlation with the magnetic characterization is discussed in this paper.

Experimental Section

Polycrystalline samples of $BiMnO_3$ were synthesized by using a high-pressure multianvil apparatus in a wide range of experimental conditions. Pressure, temperature, and reaction time were varied from 40 to 50 kbar, from 723 to 1023 K, and from 3 to 20 h, respectively. As starting material a mixture of bismuth oxide (Bi_2O_3; Aldrich, 99.99%) and manganese(III) oxide (Mn_2O_3; Aldrich, 99.999%), in a molar ratio ranging from 0.8 to 1.0, was used. Powder reagents were carefully mixed and ground, palletized (∅ = 5 mm), encapsulated in a Pt foil (50−100 μm thick), inserted into an octahedral MgO cell assembly, and placed in a 6/8-type multianvil apparatus (Rockland Research Corp.). After the application of the desired pressure (increasing rate 120 bar/min), the sample was heated at the reaction temperature at a rate of 50 °C/min. After reaction the sample was quenched to room temperature (RT), and finally the pressure was slowly released (−50 bar/min). The reaction temperature was monitored by a Pt/Pt−Rh10% thermocouple, in direct contact with the capsule. By several calibrations previously performed on the multianvil apparatus, both temperature and pressure gradients can be considered negligible inside the capsule volume during the experiment.

The prepared samples were characterized by XRPD, performed by using a Thermo ARL X'tra diffractometer, equipped with Cu Kα radiation ($\lambda = 1.54178$ Å) and a Thermo Electron solid-state detector. Collecting conditions were typically 0.01−0.02° steps and 5−10 s/step counting times. Structural data were analyzed by Rietveld refinement using the GSAS program.[19]

Transmission electron microscopy (TEM) analyses were performed using a Philips Tecnai F20 working at 200 kV and equipped with an energy dispersion X-ray (EDX) spectrometer. The specimens were prepared by grinding the samples in isopropyl alcohol and by evaporating the suspension on a copper grid covered with a holey carbon film. Selected area electron diffraction (SAED) patterns and HREM images were collected by a Gatan slow scan CCD camera.

The magnetization (M) was measured in a magnetic field up to 5 T in the temperature range 5−200 K with a commercial superconducting quantum device (SQUID) magnetometer (Quantum Design). Magnetization curves were measured in both field-cooling (FC) and zero-field-cooling (ZFC) modes.

Results and Discussion

Optimization of the Synthesis Conditions. In the first step a polycrystalline sample of $BiMnO_3$ was synthesized in the experimental conditions reported by Chiba et al.[16] Powder reagents were reacted at 873 K at 40 kbar for 3 h, then the temperature was quenched, and the pressure was slightly released. A careful observation by optical microscopy of the reacted sample revealed a nonhomogeneous material, with small and well-defined white crystalline islands embed-

(12) Kimura, T.; Kawamoto, S.; Yamada, I.; Azuma, M.; Takano, M.; Tokura, Y. *Phys. Rev.* **2003**, *B67*, 180401(R).
(13) Moreira dos Santos, A. F.; Parashar, S.; Raju, A. R.; Zhao, Y. S.; Cheetham, A. K.; Rao, C. N. R. *Solid State Commun.* **2002**, *122*, 49.
(14) Sharan, A.; Lettieri, J.; Jia, Y.; Tian, W.; Pan, X.; Schlom, D. G.; Gopalan, V. *Phys. Rev.* **2004**, B *69*, 214109.
(15) Sharan, A.; An, I.; Chen, C.; Collins, R. W.; Lettieri, J.; Jia, Y.; Schlom, D. G.; Gopalan, V. *Appl. Phys. Lett.* **2003**, *83*, 5169.
(16) Chiba, H.; Atou, T.; Faqir, H.; Kikuchi, M.; Syono, Y.; Murakami, Y.; Shindo, D. *Solid State Ionics* **1998**, *108*, 193.
(17) Atou, T.; Chiba, H.; Ohoyama, K.; Yamaguchi, Y.; Syono, Y. *J. Solid State Chem.* **1999**, *145*, 639.
(18) Faqir, H.; Chiba, H.; Kikuchi, M.; Syono, Y.; Mansori, M.; Satre, P.; Sebaoun, A. *J. Solid State Chem.* **1999**, *142*, 113.
(19) Larson, A.; von Dreele, R. B. *General Structure Analysis System (GSAS)*; Report LAUR 86-748; Los Alamos National Laboratory: Los Alamos, NM, 1994.

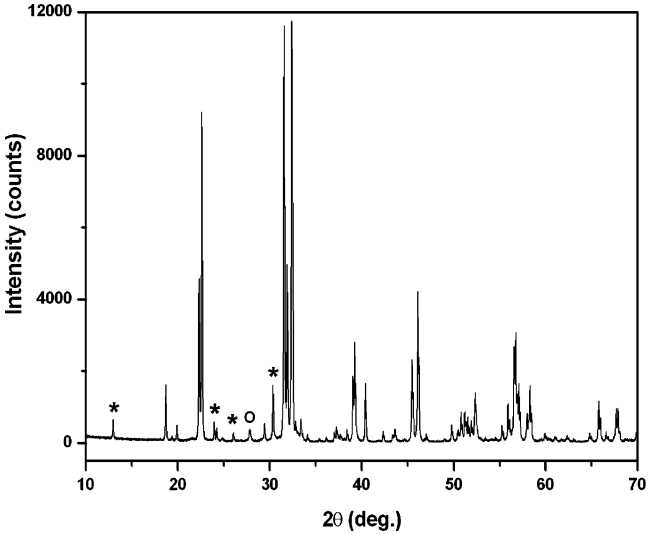

Figure 1. XRPD pattern of a $BiMnO_3$ sample prepared by 20 h of reaction at 723 K and 40 kbar. The main peaks of the impurity phases $Bi_2O_2CO_3$ and $Bi_{12}MnO_{20}$ are indicated by asterisks and an open circle, respectively.

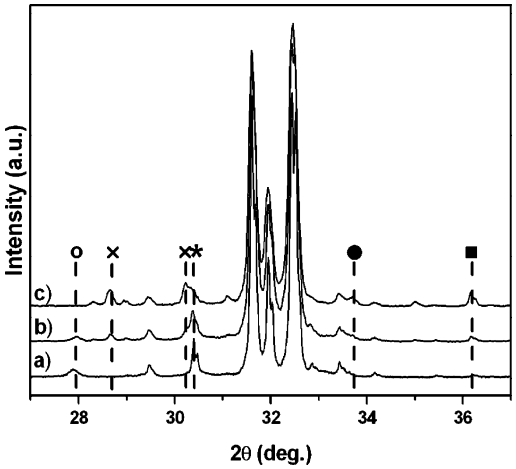

Figure 2. Comparison of the impurity peaks in the XRPD patterns of samples prepared in the same conditions (see the text) starting from a different nominal composition, $Bi_{1-x}MnO_3$: (a) $x = 0.0$; (b) $x = 0.1$; (c) $x = 0.2$. The identified impurity phases are $Bi_2O_2CO_3$ (asterisk), $Bi_{12}MnO_{20}$ (open circle), $Bi_2Mn_4O_{10}$ (times signs), Mn_3O_4 (square), and Mn_3O_4 hp form (closed circle).

ded quite uniformly in a dark-gray sintered cylinder. XRPD analysis showed that the sample mainly consisted of $BiMnO_3$, with contamination by bismuth oxycarbonate ($Bi_2O_2CO_3$) and traces of $Bi_2Mn_4O_{10}$. The presence of similar impurities was not surprising. Polycrystalline specimens of bismuth manganite have been prepared in a wide range of pressure (from 25 to 60 kbar), but the product was never found pure. As shown in Figure 1, the principal impurities usually detected are bismuth oxycarbonate and to a less extent $Bi_{12}MnO_{20}$, $Bi_2Mn_4O_{10}$, and manganese oxides.

$Bi_2O_2CO_3$ is an orthorhombic phase[20] ($a \approx c \approx 5.47$ Å and $b = 27.32$ Å), with a layered structure, easily stabilized at high pressure. $Bi_2O_2CO_3$ is formed, inside the metallic capsule, mainly by CO_2 contamination from the graphite heater of the multianvil apparatus; as reported in the literature,[21] attempts to synthesize $BiMnO_3$ without the use of a metallic protection led to complete conversion of bismuth oxide to oxycarbonate, without formation of the perovskite. When a metallic protection is used, the formation of $Bi_2O_2CO_3$ is strongly reduced, but not completely avoided, owing to microcracks, which are formed in the platinum capsule during the high-pressure heating process. On the other hand, also the possible contamination of the surface of the starting oxides (in particular of bismuth oxide) by atmospheric CO_2 should be taken into account, the reaction being performed in a confined and theoretically closed volume. We attempted, without appreciable results, to reduce the oxycarbonate contamination by preheating Bi_2O_3 at ambient pressure above the decomposition temperature of the oxycarbonate (873 K) before the perovskite synthesis. The unique result was the reduction of the reaction kinetics, connected with the decrease in surface area produced by the preheating. Therefore, we concluded that, at least until graphite heaters are used, a strong limitation of the oxycarbonate contamination, but not the obtainment of a real pure phase, should be considered as the main goal of the synthesis process. Different experiments were carried out, by changing the conditions, in particular the applied pressure, temperature, and reaction time. The best results, in terms of limited oxycarbonate contamination, were obtained by keeping the applied pressure at 40 kbar and reducing the reaction temperature to 723 K (increasing at the same time the reaction time to 20 h, to compensate the lower reactivity), with the sample encapsulated in a 50 μm thick Pt foil. In these conditions the oxycarbonate contamination, determined by Rietveld analysis of the final XRPD patterns, was found to decrease from 10% in moles, the typical value of a synthesis carried out at 873 K, to 2−3%.

As mentioned before, the synthesis at high pressure never resulted in a single phase, independently of the experimental conditions. Accurate analysis of the XRD patterns revealed that in all cases the impurities consist mainly of bismuth-rich compounds ($Bi_2O_2CO_3$, $Bi_{12}MnO_{20}$), which seem to be not adequately compensated by segregation of manganese-rich phases ($Bi_2Mn_4O_{10}$, Mn_2O_3, or Mn_3O_4), apparently leading to a Bi-deficient perovskite. This induced us to investigate the compositional stability limit of the perovskite structure by changing the starting stoichiometry. The synthesis of compounds with the formula $Bi_{1-x}MnO_3$ ($0 \le x \le 0.2$) was carried out at 40 kbar and 873 K, for about 20 h. These preparative conditions were chosen to increase the reactivity of the reagents to minimize the occurrence of incomplete reaction. The room temperature XRD patterns of the prepared samples are shown in Figure 2. The decrease of the Bi/Mn ratio preserves the perovskite growth: there is no evidence for structural transformation of the perovskite by increasing x, and no significant change in the lattice parameters is observed. By decreasing the Bi/Mn ratio, a small reduction of the always present bismuth oxycarbonate content is observed, whereas Bi-rich impurities are substituted by Mn-rich ones: $Bi_{12}MnO_{20}$ is replaced by $Bi_2Mn_4O_{10}$ just for $x = 0.1$, and the main diffraction peaks of manganese oxides become more and more detectable. This suggests the global stoichiometry of the perovskite to be independent of the starting composition, a hypothesis supported by magnetic

(20) Graves, C.; Blower, S. K. *Mater. Res. Bull.* **1988**, *23*, 1001.
(21) Atou, T.; Faqir, H.; Kikuchi, M.; Chiba, H.; Syono, Y. *Mater. Res. Bull.* **1998**, *33*, 289.

measurements showing the same T_C for all the samples, independently of the experimental conditions and starting stoichiometry. Owing to the polyphasic nature of the prepared samples that prevents chemical analyses, the determination of the chemical composition of the perovskite was performed by energy dispersion X-ray (EDX) analysis coupled with TEM. The results indicated a Bi/Mn ratio close to one for all the examined perovskite grains independently of the preparative conditions. This allows the conclusion that even the nominally stoichiometric samples should contain unreacted manganese oxide, whose absence in the XRPD patterns could be justified by taking into account its low scattering power, in comparison with that of Bi-containing phases, and a reduced grain size.

The analysis of the diffraction profile indicated that the microstructure is influenced to some extent by the different starting stoichiometry. The full width at half-maximum (FWHM) increases by decreasing the Bi content, indicating that the excess of manganese oxide acts as a crystallization inhibitor in the sintering process.

X-ray Structural Analysis at Room Temperature. A deep structural characterization of all the prepared samples was carried out by X-ray powder diffraction, selected area electron diffraction, and high-resolution electron microscopy.

The crystal structure of the $BiMnO_3$ perovskite was refined by the Rietveld method on powder diffraction data collected with Cu Kα radiation (2θ range 10−120°, step 0.01°, and counting time 10 s/step) on a sample prepared in different conditions. The monoclinic structure previously reported[17] in space group *C*2 (No. 5) was used as a basic model. Owing to the unavoidable presence of $Bi_2O_2CO_3$ impurities in all the prepared samples, perovskite was refined by taking into account the contribution of the oxycarbonate to the diffraction patterns. Refined parameters were the background, relative fraction between the two phases, profile parameters, coordinates, occupancy, and isotropic thermal factors. The results of the refinements, all confirming the monoclinic structure as gained by neutron powder diffraction, are comparable for samples prepared in different conditions and starting from different compositions. This agrees with the hypothesis that the stoichiometry of the $BiMnO_3$ perovskite is independent of the preparative conditions. The final Rietveld plot of a typical refinement (sample synthesized at 723 K and 40 kbar) is shown as an example in Figure 3.

TEM Investigations. Differently from XRPD, where the monoclinic *C*2 model explains all the detectable peaks in the experimental diffraction pattern, the TEM analysis clearly indicated the presence of a second polymorph, always derived from the perovskite, in all the examined samples (the same used for XRPD analysis).

It must be pointed out that TEM characterization of $BiMnO_3$ is complicated by the presence of a severe twinning arising on one side from its pseudocubic nature and on the other side from the probable occurrence of phase transition(s) during the cooling to room temperature and the pressure release process at the end of high-pressure synthesis. Even by working in the selected area mode, by closing the diaphragm to reduce as much as possible the illuminated area, the occurrence of single-domain ED patterns is rather rare.

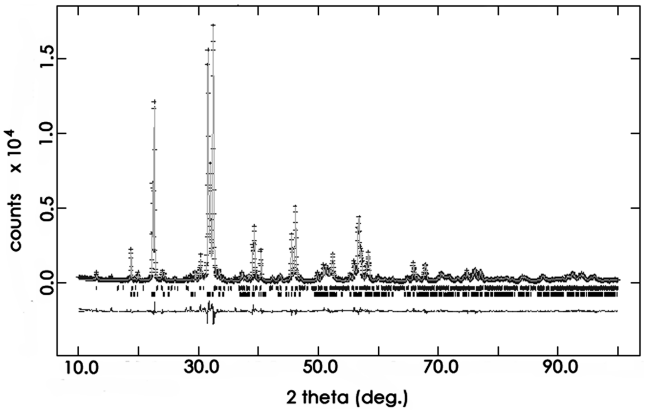

Figure 3. Final Rietveld plot obtained by refinement of the XRD pattern of a $BiMnO_3$ sample prepared at 723 K and 40 kbar. Cell parameters a = 9.5421(2) Å, b = 5.6114(1) Å, c = 9.8590(2) Å, and β = 110.628(1)°, R_p = 7.23%, and R_{F^2} = 6.14%.

For this reason and for a better comparison of diffraction patterns produced by different polymorphs, we will use, in the figures, indexes and zone axes related to their fundamental perovskite substructure.

Figure 4 shows some ED patterns that agree with the reported structure:[17] the fundamental perovskite reflections are coupled with commensurate satellites, which originate from the monoclinic superlattice. As discussed before, the occurrence of similar patterns was quite rare in our TEM observations. The typical situation, consisting of simultaneous diffraction from a few domains with different orientations and/or modulations, is depicted in Figure 5. These ED patterns are mostly characterized by the appearance of additional modulation satellites, still commensurate to the perovskite sublattice but not explainable in terms of the C-centered monoclinic superstructure. Owing to the twinning domains affecting the samples, the fundamental spots of the perovskite cell are broadened or, more usually, doubled (or tripled); in contrast, the modulation satellites are often well defined, as expected if produced by a single crystal domain. Taking into account the ED patterns simulated on the basis of the known structure (hereinafter denoted as **I**), the composite experimental patterns could be deconvoluted into the single contributions, as shown in Figure 5, suggesting the existence of a second polymorphic form of the $BiMnO_3$ phase (hereinafter denoted as **I***), whose domains grow isooriented (in terms of the perovskite structure) with **I** in the samples.

This idea was reinforced by HREM studies, where single domains showing the typical features either of the former or of the latter form could be isolated. Figure 6 shows a twinning boundary between two domains, each one referring to a different polymorph, as shown by the Fourier transforms in the insets.

As shown in Figure 5, the indexing of the composite diffraction patterns requires quadrupling in any direction the periodicity of the fundamental perovskite. This forces consideration of a redundant pseudocubic perovskite supercell (PS) defined, as shown in Figure 7a, by $a_{PS} = 4a_P$. In this new cell setting, the discrimination between satellite reflections produced by polymorphs **I** and **I*** becomes quite simple, if the diffraction symmetry is taken into account. In

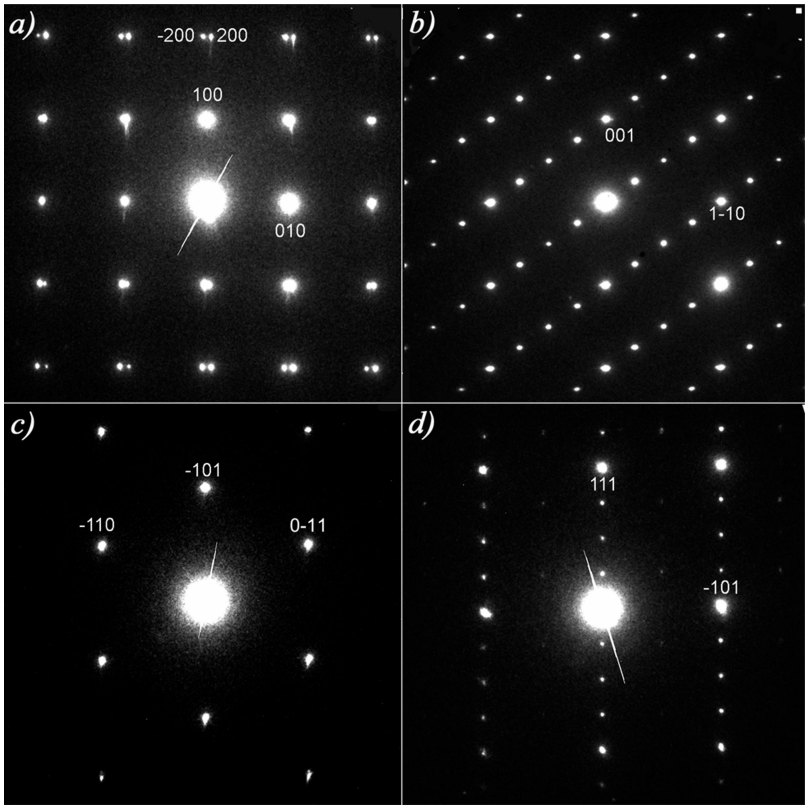

Figure 4. SAED patterns on different zone axes for the polymorph **I** of $BiMnO_3$: (a) $[001]_P$; (b) $[110]_P$; (c) $[111]_P$; (d) $[1\ -2\ 1]_P$. Zone axes and indexes refer to the fundamental perovskite cell. The presence of a reflection twin (the twin plane is (010)) is evidenced in (a).

fact, as shown in Figure 7b, the relationship between the PS and **I** cells leads the **I** satellites to follow, in the PS setting, the extinction rule of a F-centered lattice ($h + k$, $h + l$, $k + l = 2n$). In contrast, the satellites produced by polymorph **I*** are consistent with an I-centered lattice ($h+k+l = 2n$), making the discrimination in many cases straightforward. The unique doubtful cases are represented by patterns showing only $2h2k2l$ reflections (with all even indexes both the centering conditions are simultaneously satisfied), but this is fortunately limited to very few and well-known projections of polymorph **I**.

Following this idea, meticulous and patient work performed in SAED allowed collection of diffraction patterns of the new polymorph (some example are shown in Figure 8) from single-grain domains. A strong facilitation came from the change in microstructure produced by the reduction of the synthesis temperature of $BiMnO_3$ to 723 K. The samples prepared at this temperature were shown by TEM characterization to be less affected by twinning than those prepared at 873 K. Nevertheless, whereas XRD patterns remained fully interpretable on the basis of the unique polymorph **I**, polymorph **I*** became dominant in the ED patterns, for which a thin edge region of the samples is usually examined. The successful acquirement of single-grain ED patterns in several zone axes led to the determination of the lattice parameters of polymorph **I***, which was performed with the QED software.[22] The unit cell was found to be $a = 13.62$ Å, $b = 13.66$ Å, $c = 13.66$ Å, $\alpha = 110°$, $\beta = 108.8°$, and $\gamma = 108.8°$. This pseudorhombohedral cell, as shown in Figure 7c, corresponds to the primitive cell of a pseudocubic I-centered PS lattice, in agreement with the systematic absences observed in ED patterns for this cell setting.

The structural description of **I*** requires a cell which is 32 times larger in volume than the simple perovskite and 4 times larger than the C-centered monoclinic cell of **I**. The cell is related to a fundamental perovskite with $a \approx c \approx 3.97$ Å, $b \approx 3.92$ Å, $\alpha \approx 90.7°$, $\beta \approx 90.4°$, and $\gamma \approx 89.3°$: with respect to the distortion of the cubic perovskite observed for polymorph **I**, the "two shorter axes and a longer one" condition is turned into "two longer axes and a shorter one" for **I***. It must to be noticed that the diffraction patterns of **I***, despite the reduced symmetry of the unit cell, show generally an apparent higher symmetry (pseudocubic) if only the diffracted intensities and not the geometric relationships among the reciprocal lattice vectors are considered. Together with the relative weakness of the superstructure reflections, this suggests a small deviation from the ideal perovskite structure, at least for what concerns the heavy Bi atoms.

The existence of a second polymorph was taken into account by Chiba et al.,[16] in a preliminary structural study of $BiMnO_3$, to explain an experimental ED pattern not consistent with the C-centered monoclinic cell they proposed in the paper. On the basis of our data, this SAED pattern is a typical pattern of polymorph **I***, taken on the $[100]_P$ zone axis. The authors connected this second polymorph to the cell given a long time ago by Bokov et al.[23] for $BiMnO_3$ (triclinic, lattice parameters $a = c = 7.86$ Å, $b = 7.98$ Å, $\alpha = \gamma = 91.67°$, and $\beta = 90.97°$, which can be transformed

(22) Belletti, D.; Calestani, G.; Migliori, A.; Gemmi, M. *Ultramicroscopy* **2000**, *81*, 57.

(23) Bokov, V. A.; Myl'nikova, I. E.; Kizhaev, S. A.; Bryzhina, M. F.; Grigoryan, N. A. *Sov. Phys. Solid State* **1966**, *7*, 2993.

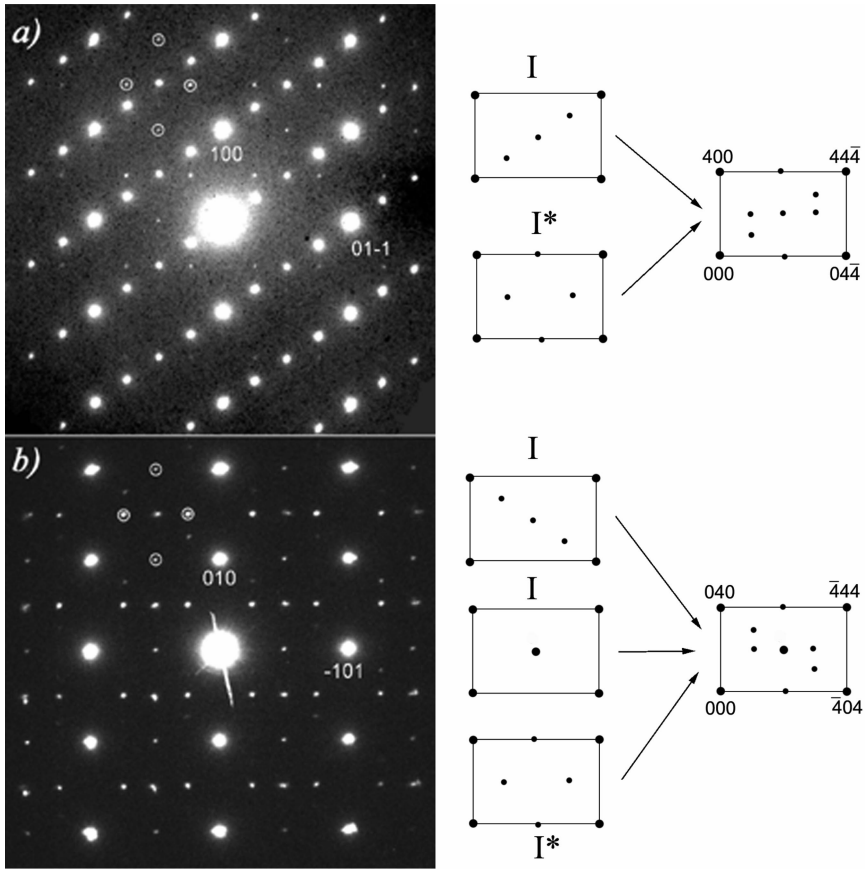

Figure 5. Typical examples of SAED patterns of a $BiMnO_3$ sample, taken on $[011]_P$ (a) and $[101]_P$ (b) zone axes, revealing a composite nature based on different diffraction domains and structural modulations. As shown on the right, the full indexing of the diffraction patterns, whose deconvolution involves two and three diffraction domains for (a) and (b), respectively, requires quadrupling the *hkl* indexes. The diffraction domain, denoted as **I*** and common to both patterns, corresponds to the reflections circled in the experimental images, which cannot be indexed on the basis of polymorph **I** (see the text for more details).

into a monoclinic C-centered cell with a double volume). However, neither the published ED pattern nor the ones we collected are consistent with the reported cell. In further structural studies of the same group, the second polymorph was no longer mentioned, probably being considered an impurity with negligible or occasional character. Our study clearly demonstrates not only that this phase is always present, but also that it becomes dominant in TEM characterization for particular samples (the ones prepared at lower temperature) or in particular experimental conditions, as, for example, on $[100]_P$ zone axis. In fact, all the SAED patterns (tens) collected on this zone axis for different samples, as well as the corresponding HREM images (an example is shown in Figure 9), showed the typical modulation features of polymorph **I***.

A first hypothesis to justify the discrepancy between XRD and ED characterizations could be the formation of polymorph **I*** in the microscope under the excitation produced by the electron beam. However, this hypothesis is in contrast with the experimental results. In fact, no change was observed, in both ED and HREM, by keeping the same region under observation for a long time. On the other hand, owing to the semiconductor nature of $BiMnO_3$, heating of the sample under irradiation, leading to a phase transition, can be excluded (the first phase transition occurring on heating polymorph **I** was observed above 483 K[18]). The unique hypothesis that agrees with the experimental observation is the confinement of polymorph **I*** at the surface of the grains. This, on one side, could explain the observation of **I*** in ED and HREM analysis, which are typically performed on the thin region near the sample edge. At the same time this could also explain the "absence" of **I*** in XRD patterns, by taking into account a certain degree of mimicry produced by the topotactic growth of this phase on **I** and the thickness of the surface layer, which could be in most cases below the coherence length of the X-ray radiation.

It is quite interesting to note that, once the sample has been reheated at high temperature and ambient pressure just below the irreversible transition to the tetragonal phase that precedes the thermal decomposition of $BiMnO_3$,[18] polymorph **I*** disappears. In fact, after this treatment, no trace of the phase was found in SAED patterns collected at room temperature that show uniquely the typical modulation features of **I**. Changes were observed also in XRPD patterns, showing still the typical diffraction profile of polymorph **I** but, in a systematic way, different relative intensities of the main perovskite peaks. On one side the observed profile difference could be interpreted in terms of the contribution of polymorph **I*** to the main reflections of the perovskite; however, the occurrence of a reversible phase transition at 483 K during the heating and cooling processes must be taken into account, and the observed discrepancy could be interpreted also in terms of microstructural changes induced by the phase transition.

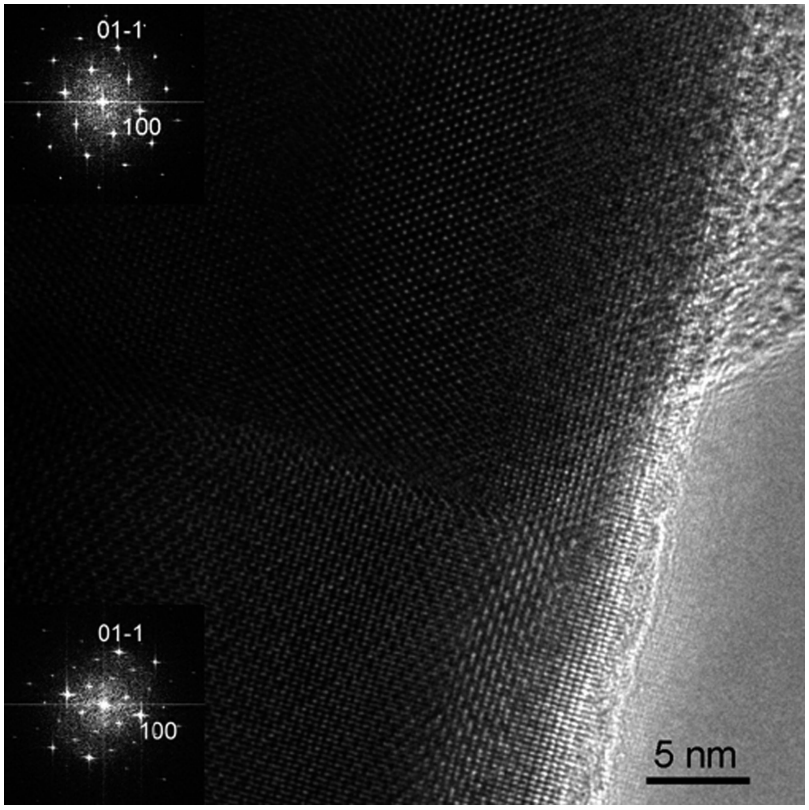

Figure 6. HREM image taken on the $[011]_P$ zone axis, showing the twinning boundary between two different polymorphs. The corresponding Fourier transforms, shown in the insets, give diffraction patterns in analogy with two components of Figure 5b.

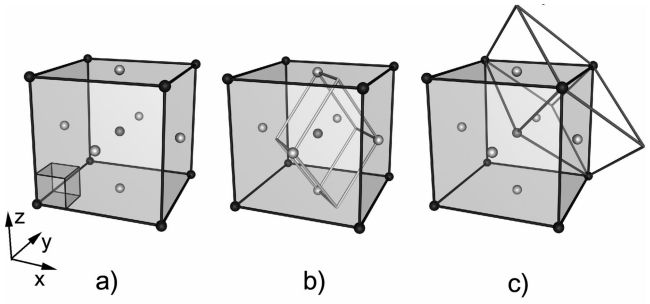

Figure 7. Redundant pseudocubic perovskite superstructure PS ($a_{PS} = 4a_P$) and its relationship with (a) the basic perovskite cell, (b) the monoclinic cell of polymorph **I**, and (c) the pseudorhombohedral cell of polymorph **I***. In (b) and (c) the **I** and **I*** cells are translated to a permitted origin to better visualize the corresponding F- or I-centered character of their descriptions on the PS basis. The transformation matrixes from **I** and **I*** to PS are (1 −2 1/1 0 −1/1 2 1) and (1 0 1/0 1 1/−1 −1 0), respectively.

The disappearance of **I*** on heating at ambient pressure, clearly evidenced by ED, suggests that **I*** would be a higher energy polymorph, which converts kinetically to **I**, once a sufficient temperature has been achieved. This hypothesis is in agreement with the experimental observation of a large amount of **I*** in the samples prepared at lower temperatures and suggests that the presence of **I*** in the as-prepared samples could be ascribed to the decrease of the transformation kinetics at high pressure. On the other side, since **I*** is formed at the edge of the monoclinic crystallites, a variation of its chemical composition with respect to **I** (enrichment or deficiency in oxygen or cationic deficiency) could be taken into account. We performed EDX microanalysis on several $BiMnO_3$ grains with comparable results, but this cannot be considered definitive evidence of a unique composition, owing to the insensitiveness of the technique toward oxygen and to experimental errors, which could mask small deviations in the cationic content. We also performed thermal retreatment of the as-prepared sample in both oxidizing and reducing atmospheres, always observing the disappearance of **I***. Therefore, since no definitive conclusion on the phase stoichiometry can be drawn, the term polymorph, to indicate the **I*** structural variant, is used in this work in a broad sense.

Magnetic Characterization. Magnetic investigations proved $BiMnO_3$ samples synthesized under high pressure to be a mixture of different polymorphs, each one detectable because of a different magnetic behavior at low temperature.

The magnetization behavior (field cooling and zero-field cooling of a typical $BiMnO_3$ sample) is shown in Figure 10. According to the structural investigation, the major magnetic contribution belongs to the well-known and widely investigated ferromagnetic form **I**: both field cooling and zero-field cooling show the typical ferromagnetic characteristic below the Curie temperature (T_C = 99 K). The critical temperature is the same for all the samples synthesized under different experimental conditions (firing temperature or pressure), and the experimental results are in agreement with the literature; the reported[24] spontaneous magnetic moment is 2.6 μ_B at 77 K and 1 T, whereas at 5 K and 5 T its value (3.6 μ_B) is close to the ideal value expected for Mn^{3+} ions (4 μ_B); our measurements gave slightly lower values (2.5 μ_B at 78 K and 2 T and 3.2 μ_B at 5 K and 5 T), but it must be pointed out that the estimation of the real amount of the magnetic phase is complicated by the polyphasic nature of the samples.

(24) Chiba, H.; Atou, T.; Syono, Y. *J. Solid State Chem.* **1997**, *132*, 139.

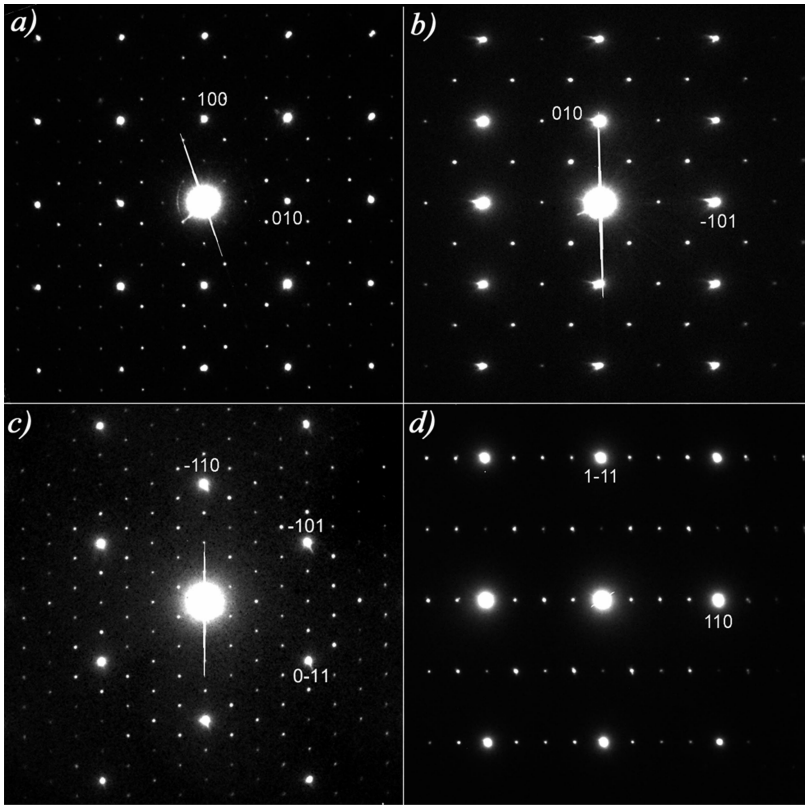

Figure 8. SAED patterns in different zone axes for the polymorph **I*** of $BiMnO_3$: (a) $[001]_P$; (b) $[101]_P$; (c) $[111]_P$; (d) $[-1\ 1\ 2]_P$. Zone axes and indexes refer to the fundamental perovskite cell.

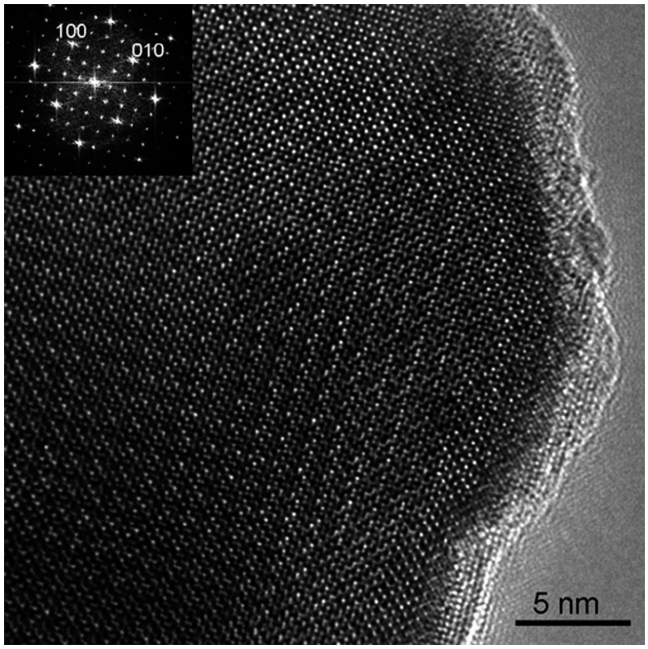

Figure 9. HREM image taken on the $[001]_P$ zone axis, showing the typical modulation features of polymorph **I***. The Fourier transform of the image is shown in the inset.

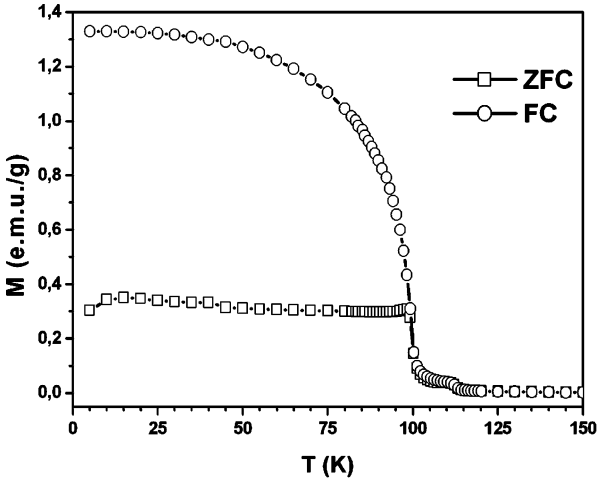

Figure 10. Magnetization vs temperature for a $BiMnO_3$ sample prepared at 743 K and 40 kbar (20 h): FC and ZFC refer to measurements performed by field cooling (10 Oe) and zero-field cooling, respectively.

As shown in Figure 10, all the measured samples display a further magnetic contribution with a critical temperature of 107 K, which is independent of the eventual presence of other known magnetic impurities (Mn_3O_4, $Bi_2Mn_4O_{10}$), which give ferri- or antiferromagnetic contribution at low temperature. On the basis of the structural characterization, this contribution could be related to the presence of the second polymorph detected by ED in the samples. To confirm this hypothesis, a sample was prepared at the lowest possible temperature (723 K, to maximize the content in polymorph **I***) and successively reheated at 753 K in nitrogen (to eliminate this phase). Figure 11 shows a comparison of the magnetic measurements performed on the as-prepared sample and after the thermal treatment. The magnetic contribution at 107 K, revealed in the as-prepared sample, disappears after the second treatment. Comparative XRPD and TEM analysis revealed the disappearance of polymorph **I*** as the unique variation produced in the sample by the thermal treatment, suggesting a connection between the magnetic contribution at 107 K and the new polymorph, which has been confirmed in further experiments. Because of the small quantity of **I***

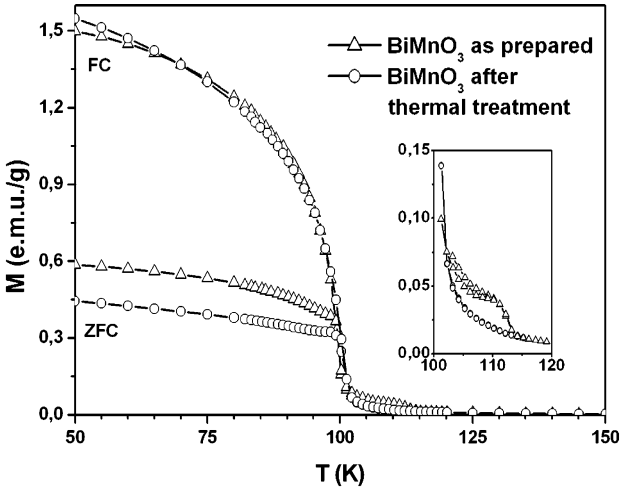

Figure 11. Comparison of magnetization vs temperature for a $BiMnO_3$ sample prepared at 723 K and 40 kbar (20 h) before and after a further heating at ambient pressure to 753 K (20 K/min): FC and ZFC refer to measurements performed by field cooling (10 Oe) and zero-field cooling, respectively. An enlargement of the transition region is shown in the inset.

in each specimen, its magnetic nature is not yet completely understood, its contribution being mainly hidden below 100 K by the dominant presence of the ferromagnetic phase **I**.

Conclusions

$BiMnO_3$ polycrystalline samples, synthesized in a wide range of experimental conditions (high pressure−high temperature), were investigated by electron diffraction and HREM. This study evidenced the existence of a second polymorph, which coexists as a minor phase with the well-known monoclinic form (**I**) at room pressure and temperature. Like **I**, this second form (**I***) has a distorted perovskite basic cell, but is described by a different superstructure with triclinic (pseudorhombohedral) symmetry. The distortion of the basic perovskite cell is similar to that observed by heating **I** above 483 K, where a reversible monoclinic−monoclinic phase transition[18] takes place, but the symmetries of the two structures differ completely.

The existence of polymorphism in $BiMnO_3$ at room temperature was previously suggested by Chiba et al.,[16] on the basis of an experimental ED pattern not consistent with the monoclinic form, but no further investigations were carried out due to the fact that the **I*** form is usually not detectable by other diffraction techniques. By ED and HREM we systematically found **I*** in all the examined samples, in particular in those prepared at lower temperatures, where its contribution to ED becomes dominant. Our investigations suggest that the **I*** phase is confined at the grain surface, giving an explanation for the discrepancy observed among different diffraction techniques. It is possible to obtain the pure **I** phase, since the **I*** phase disappears after reheating of the samples at ambient pressure just below the irreversible transition to the tetragonal phase (763 K), which precedes the thermal decomposition of $BiMnO_3$.[18] This suggests that **I*** would be a higher energy polymorph, which converts kinetically to **I**, once a sufficient temperature has been achieved. A comparison of the magnetic behaviors of as-prepared and reheated samples allows association of the **I*** phase with a secondary magnetic transition observed at 107 K in all the as-prepared samples, a few degrees above the magnetic transition of polymorph **I** measured at 99 K. Despite the experimental conditions generally used in the literature for the preparation of $BiMnO_3$ falling in the range used in this work, it is plausible to consider the occurrence of polymorphism at RT a common feature of the samples used to study its multiferroic nature. However, this does not impugn the results of these studies, **I** in any case being the dominant phase.

As evidenced in previous works,[10,11] the ferromagnetic nature of **I** is strictly linked to the distortion of the perovskite structure produced by the stereoactive lone pair of bismuth ions. It is therefore interesting to note that the rearrangement of bismuth ions in form **I***, showing a quite different symmetry, still leads to a magnetic transition at a temperature close to that of the previous case. The study of the crystal structure and of the electric and magnetic nature of this polymorph could give important contributions to the comprehension of the multiferroic nature of the *C*2 monoclinic bismuth manganite and of the origin of ferroelectricity in the system, which is not yet completely understood. All these investigations require isolation of the **I*** phase. Further work is in progress to check different reaction paths in the $T-P$ diagram to find the conditions in which this phase is formed during the preparation process.

Acknowledgment. We thank Dr. Franca Alberini (CNR-IMEM) for preliminary magnetic investigations and Dr. Simone Fabbrici (CNR-IMEM) for his collaboration.

CM048250S